Microbe-focused glycan array screening platform

Andreas Geissner[a,b,1], Anika Reinhardt[a,b,2], Christoph Rademacher[a,b], Timo Johannssen[a,b], João Monteiro[c], Bernd Lepenies[a,b,c], Michel Thépaut[d,e,f], Franck Fieschi[d,e,f], Jana Mrázková[g], Michaela Wimmerova[g], Frank Schuhmacher[a,b], Sebastian Götze[a,b,3], Dan Grünstein[a,b], Xiaoqiang Guo[a,b,4], Heung Sik Hahm (함흥식)[a,b,5], Jeyakumar Kandasamy[a,6], Daniele Leonori[a,7], Christopher E. Martin[a,b,8], Sharavathi G. Parameswarappa[a,9], Sandip Pasari[a,10], Mark K. Schlegel[a,11], Hidenori Tanaka[a,12], Guozhi Xiao[a,13], You Yang[a,14], Claney L. Pereira[a,15], Chakkumkal Anish[a,16], and Peter H. Seeberger[a,b,17]

[a]Department of Biomolecular Systems, Max Planck Institute of Colloids and Interfaces, 14424 Potsdam, Germany; [b]Institute of Chemistry and Biochemistry, Freie Universität Berlin, 14195 Berlin, Germany; [c]Immunology Unit and Research Center for Emerging Infections and Zoonoses, University of Veterinary Medicine Hannover, 30559 Hannover, Germany; [d]Université Grenoble Alpes, Institut de Biologie Structurale, F-38044 Grenoble, France; [e]CNRS, Institut de Biologie Structurale, F-38044 Grenoble, France; [f]Commissariat à l'Énergie Atomique et aux Énergies Alternatives, Institut de Biologie Structurale, F-38044 Grenoble, France; and [g]Central European Institute of Technology, Masaryk University, 625 00 Brno, Czech Republic

Edited by Michael L. Klein, Temple University, Philadelphia, PA, and approved December 14, 2018 (received for review January 16, 2018)

Interactions between glycans and glycan binding proteins are essential for numerous processes in all kingdoms of life. Glycan microarrays are an excellent tool to examine protein–glycan interactions. Here, we present a microbe-focused glycan microarray platform based on oligosaccharides obtained by chemical synthesis. Glycans were generated by combining different carbohydrate synthesis approaches including automated glycan assembly, solution-phase synthesis, and chemoenzymatic methods. The current library of more than 300 glycans is as diverse as the mammalian glycan array from the Consortium for Functional Glycomics and, due to its microbial focus, highly complementary. This glycan platform is essential for the characterization of various classes of glycan binding proteins. Applications of this glycan array platform are highlighted by the characterization of innate immune receptors and bacterial virulence factors as well as the analysis of human humoral immunity to pathogenic glycans.

glycan arrays | microbial antigens | immune receptors | antiglycan antibodies | bacterial lectins

Carbohydrates are abundant in all kingdoms of life and interact with glycan binding proteins (GBPs) in the context of many important cellular processes including fertilization (1) and cell adhesion and motility (2) as well as immunity and host–pathogen recognition (3). To better understand protein–glycan recognition, the specificities of GBPs for many structurally diverse glycans must be determined since even minor structural changes greatly influence GBP binding (4–6). Linear and branched glycans can be assembled from a large set of monosaccharide building blocks using various modes of connectivity (7, 8), requiring high-information-yielding analytical techniques that probe many GBP–glycan interactions at once.

Glycan arrays are excellent tools for glycan binding analysis due to their ability to interrogate a multitude of binding events quickly using limited amounts of sample (4, 9). Arrays produced by the surface attachment of well-defined synthetic glycans enable the elucidation of binding events with atomic resolution. Synthetic glycan arrays have been key in assigning carbohydrate specificities to numerous GBPs ranging from soluble proteins such as toxins and immune lectins to microbial and mammalian surface receptors (4, 5, 10, 11). To date, collections of synthetic glycans for microarray experiments have contained primarily or exclusively mammalian carbohydrates (4), and such large collections are also needed for the glycans that cover the surfaces of pathogens and other microbes as these structures mediate, among other functions, recognition by immune lectins and receptors as well as biofilm formation by interaction with bacterial lectins (12–16). Antibodies directed against pathogen surface glycans hold great potential as infection markers (11, 17), and significant biological insight has already been gained from experiments using arrays printed with smaller focused collections of synthetic microbial glycans (18–22).

Significance

The interplay between glycan binding proteins and their carbohydrate ligands is fundamental to all aspects of life. Printed glycan arrays have helped to elucidate the role of glycans in many biological processes with monosaccharide resolution, particularly those of mammalian origin, over the past 15 y. Current microbial glycan arrays contain specialized small synthetic collections or isolated carbohydrates but better coverage is needed as microbes are enveloped in complex layers of carbohydrates. The chemically diverse microbial glycans play crucial roles in immunity and infectious diseases. We present an extensive synthetic glycan collection focused on microbial glycans as a tool to investigate microbial glycobiology.

Author contributions: A.G., A.R., C.R., C.L.P., C.A., and P.H.S. designed research; A.G., A.R., C.R., T.J., J. Monteiro, M.T., and J. Mrázková performed research; T.J., B.L., M.T., F.F., J. Mrázková, M.W., F.S., S.G., D.G., X.G., H.S.H., J.K., D.L., C.E.M., S.G.P., S.P., M.K.S., H.T., G.X., Y.Y., and C.L.P. contributed new reagents/analytic tools; A.G. and A.R. analyzed data; and A.G., A.R., and P.H.S. wrote the paper.

The authors declare no conflict of interest.

This article is a PNAS Direct Submission.

[1]Present address: Department of Chemistry, University of British Columbia, Vancouver, BC, Canada V6T 1Z1.

[2]Present address: Department of Life Science Frontiers, Center for iPS Cell Research and Application, Kyoto University, 606-8507 Kyoto, Japan.

[3]Present address: Universität Koblenz·Landau, Faculty 7: Natural and Environmental Sciences, 76829 Landau, Germany.

[4]Present address: Clariant Innovation Center, 65929 Frankfurt am Main, Germany.

[5]Present address: Department of Chemistry, University of Virginia, Charlottesville, VA 22904.

[6]Present address: Department of Chemistry, Indian Institute of Technology, 221005 Varanasi, Uttar Pradesh, India.

[7]Present address: School of Chemistry, University of Manchester, M13 9PL Manchester, United Kingdom.

[8]Present address: Bachem AG, 4416 Bubendorf, Switzerland.

[9]Present address: Vaxxilon Deutschland GmbH, 12489 Berlin, Germany.

[10]Present address: Indian Institute of Science Education and Research, 411008 Pune, India.

[11]Present address: Alnylam Pharmaceuticals, Cambridge, MA 02142.

[12]Present address: Oceanography Section, Science Research Center, Kochi University, Otsu 200, Nankoku City, Kochi 783-8503, Japan.

[13]Present address: State key Laboratory of Phytochemistry and Plant Resources in West China, Kunming Institute of Botany, Chinese Academy of Sciences, 650201 Kunming, China.

[14]Present address: Shanghai Key Laboratory of New Drug Design, School of Pharmacy, East China University of Science and Technology, 200237 Shanghai, China.

[15]Present address: Vaxxilon Deutschland GmbH, 12489 Berlin, Germany.

[16]Present address: Janssen Pharmaceuticals (Johnson & Johnson), Bacterial Vaccines Discovery and Early Development, 2333 CK Leiden, The Netherlands.

[17]To whom correspondence should be addressed. Email: peter.seeberger@mpikg.mpg.de.

This article contains supporting information online at www.pnas.org/lookup/suppl/doi:10.1073/pnas.1800853116/-/DCSupplemental.

Published online January 22, 2019.

To date, however, microbial glycan arrays have been created mainly from isolated carbohydrates that were derivatized for immobilization purposes (23). Depending on the experimental objective, a few (24–27), dozens (28, 29), about 150 (30, 31), and even up to 300 (32) of such isolated and characterized carbohydrate preparations have been immobilized. Shotgun glycan arrays exposing the fractionated but uncharacterized glycome of a given sample have revealed important binding information about native receptors albeit with lower resolution and structural control than synthetic arrays would allow (33, 34). In-depth binding analysis requires a combination of arrays based on synthetic and isolated carbohydrates (4, 23).

The chemical diversity of bacterial glycomes poses a significant synthetic challenge (7, 8). Here, we have combined complementary glycan synthesis strategies, including automated glycan assembly, to generate a diverse collection of glycans that contain a functionalized linker for immobilization via site-specific coupling to reactive surface groups (35) (Fig. 1). Glycans not yet accessible by automation were prepared by classical solution-phase synthesis, by chemoenzymatic synthesis, or by a combination of both (36). From this glycan collection, referred to as the Max Planck Society (MPS) glycan library, sets of glycans are selected for biological experiments (Fig. 2). The analyses of serum antiglycan antibodies, innate immune receptors, and bacterial virulence factors presented here serve as examples for the myriad of investigations that will profit from this pathogen-focused glycan array platform.

Results

MPS Glycan Library Analysis. The MPS glycan library is based on carbohydrate structures that had been prepared for numerous chemical glycobiology studies involving pathogenic cell-surface saccharides (*SI Appendix*, Tables S2 and S3). Many of the 300 mono- to eicosasaccharides in the library represent carbohydrates found on pathogenic bacteria or parasites, in addition to mammalian glycans, substructures of plant polysaccharides, or fragments thereof that are too small to be uniquely categorized (Fig. 3*A*). Some glycans, such as the Lewis blood group antigens for mammals, have been assigned to one typical group even though they are also found in other organisms. Most glycans contain a reducing end linker with a reactive primary amine but some are functionalized with a thiol linker instead (*SI Appendix*, Tables S2–S4). The reaction of amine-functionalized glycans with *N*-hydroxysuccinimide (NHS) ester activated glass surfaces that was also used for the experiments described below is a standard immobilization methodology in many laboratories (4, 34, 37–39). Immobilization via thiol groups has been used in many successful studies in our laboratory (21, 40–43). In the few cases where the reducing end is naturally modified, the linker is positioned elsewhere (44).

Calculation of diversity (45) for our library and comparison with two other microarray platforms, the Consortium for Functional Glycomics (CFG) mammalian array 5.2 and the library of Feizi at Imperial College London, resulted in very similar scores (MPS: 0.643; CFG: 0.645; Feizi: 0.641). The diversity score is the average over all dissimilarities between pairs of glycans in a given library. This pairwise dissimilarity is calculated from the overlap of all fragments (subtrees) of two glycans up to a specific length. The convergence of the diversity scores to very similar numbers of the three glycan arrays indicates that their diversity is similar. This is one approach among many to describe library diversity (45). Therefore, the focus on highly diverse microbial glycans with their high number of monosaccharide building blocks in the MPS library leads to a diversity similar to that of the other arrays even though our library is less than half the size of the two other analyzed collections. Interestingly, glycans of our library cluster both in comparison with the CFG (Fig. 3*B*) and the Feizi laboratory (*SI Appendix*, Fig. S1), suggesting complementarity of the libraries.

Glycan Microarray Preparation and Validation. The functional group on the linker determines the immobilization chemistry: amine-containing compounds are fixed on carboxylic acid NHS ester surfaces while thiols are printed on maleimide slides. Epoxy slides are used for mixed arrays on which both amine- and thio-functionalized glycans are immobilized (4, 21, 41–43, 46). In this case, glycan selection depends upon the experimental objective (Fig. 2). A generalized array, by definition reflecting as many and as diverse glycans as possible, is used for in-depth binding analysis. Targeted arrays where the available surface is split up into a higher number of identical fields that are printed with an identical selected subset of glycans allow for high-throughput analysis of many samples; here also the glycans are selected for a specific project (Fig. 2).

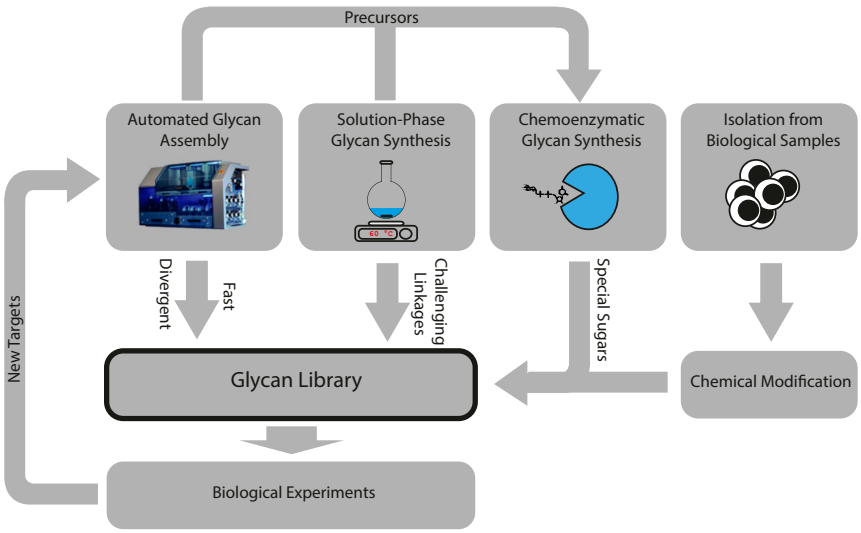

Fig. 1. Strategies to procure glycans for microarray experiments. The library contains synthetic, structurally well-defined glycans rather than carbohydrates isolated from natural sources. Automated glycan assembly allows for high diversity while reducing workload. Highly complex glycans containing difficult linkages or rare monosaccharides are accessed via complementary methods.

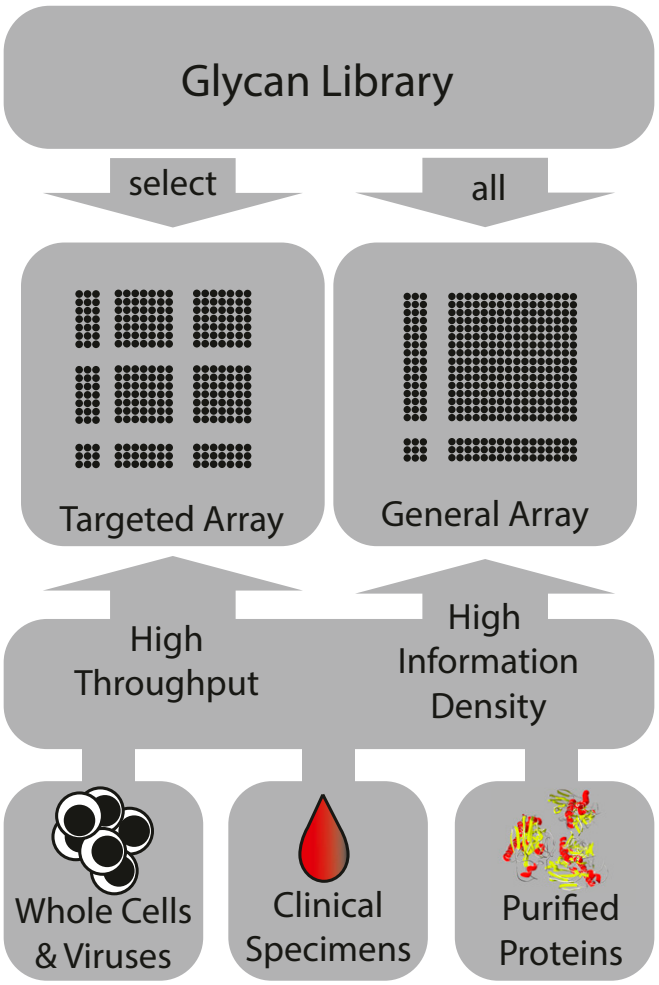

Fig. 2. Glycan selection for microarray printing. Based on the experimental design, different glycans are printed onto standard microarray slides. Special targeted arrays are designed to contain glycan subsets for high-throughput screening of various sample types. The influenza hemagglutinin structure used for illustration in the figure is based on data from ref. 88.

Printing was validated using GBPs of known specificity, plant lectins and monoclonal antibodies. Distinct binding patterns and a good correlation between expected and observed binding was seen for an array consisting of 140 aminolinker-containing glycans printed onto NHS activated glass slides probed with fluorescence-labeled plant lectins (Fig. 4 *A–C* and *SI Appendix*, Figs. S2 and S3 and Table S1). Using lectins and monoclonal antibodies, specific immobilization of 99 out of 140 printed glycans was confirmed (*SI Appendix*, Table S2). In the context of the lectins, we largely limited the specificity analysis to the nonreducing terminal monosaccharide [or disaccharide for *Ricinus communis* agglutinin (RCA120) or di-/trisaccharide for MAL I], often also including low-affinity interactions, as high lectin concentrations were used. Not only the inclusion of weaker ligands but also the limitation to the terminal saccharides potentially leads to a higher rate of "false negatives" as backbone structure and linkage position to the backbone also influence lectin binding (47, 48). The rationale behind this move was that there is no information yet available for the respective monosaccharides terminal on bacterial backbones. Indeed, for several lectins, intensities for some glycans in the expected set were quite low or no binding was seen (Fig. 4 *A–C* and *SI Appendix*, Fig. S2 and Tables S1 and S2); however, these glycans should not be excluded from further studies. In summary, 94% of the glycans for which lectin binding was expected were indeed recognized by at least one lectin for which binding was expected. Not bound at all were glycans **248** and **249** based on *Clostridium difficile* lipoteichoic acid whose terminal GlcNAc made them potential ligands of wheat germ agglutinin (WGA). The two glycans were strongly recognized by serum antibodies, though (discussed below). Recognition of the Lewis X trisaccharide on two different linkers (**154** and **176**) failed for all lectins for which we expected it, but the structure was recognized by *Bandeiraea simplicifolia* lectin I (BSL)—that probably bound to terminal β-Gal even though it is considered specific for α-Gal—and in subsequent studies (discussed below) strongly by dendritic cell-specific intercellular adhesion molecule-3-grabbing nonintegrin (DC-SIGN), as expected. Most of the remaining glycans were not bound due to a lack of specific detection reagents for many nonmammalian monosaccharides. However, we observed two interesting exceptions, to our knowledge undescribed to date, of plant lectins showing significant binding to nonmammalian glycans: (*i*) three glycans terminating in *N*-acetyl-L-fucosamine (FucNAc) were bound by the lectin UEA I that is specific for L-fucose (Fuc) and (*ii*) *N*-acetyl-D-fucosamine (D-FucNAc) **102**, the 6-deoxy derivative of *N*-acetyl-D-galactosamine (GalNAc), was bound to varying degrees by four lectins, namely *Dolichos biflorus* agglutinin (DBA), RCA120, *Sambucus nigra* lectin (SNL), and WGA. Batch-to-batch variability of the array was not assessed. The screening experiments presented below utilized this validated 140-glycan array.

Human Serum Analysis. The human serum antibody repertoire reflects major antigens encountered by the immune system during interactions with foreign organisms. Contact with numerous microbes over an individual's lifetime induces antibodies specific to many carbohydrates (17, 49, 50).

To assess the human immune response to microbial glycans, we analyzed binding of IgG from serum samples of 15 healthy individuals on the 140-glycan array and found that 126 were bound by antibodies from sera of at least one individual and 111 from three or more individuals (*SI Appendix*, Fig. S4 and Table S2). Glycans containing the 6-deoxy hexose L-rhamnose (Rha) (51), a saccharide found in many pathogens but not in mammals, produced the highest median intensities (Fig. 4*D*). Antibodies against rhamnose have been described as highly abundant in humans (52). Trirhamnoside **252**, based on the capsular polysaccharide (CPS) of a broadly drug-resistant *Klebsiella pneumoniae* strain (53, 54), displayed the highest fluorescence intensities. The rhamnosides were followed by a less-defined group with several representatives within the top 20 according to median intensity comprising glycans that contain the nonmammalian monosaccharides *N*-acetyl-D-mannosamine (ManNAc) and FucNAc/D-FucNAc. A third highly bound group encompassed oligosaccharides of D-arabinofuranose that were based on the *Mycobacterium tuberculosis* cell wall (55) (Fig. 4*D*). Binding to microbial glycans by antibodies from human samples demonstrates the suitability of our microarray platform for serum analysis.

Human Lectin Immune Receptors. In addition to profiling serum antibodies, other types of GBPs can be studied by means of the MPS glycan library, for the purpose of either initial characterization of GBPs of unknown specificity or further analysis of previously investigated GBPs. Mammalian lectin receptors of the innate immune system are of particular interest as they specifically recognize pathogen glycans leading to activation of immune processes that result in threat elimination. The human C-type lectin receptor (CLR) DC-SIGN is mainly expressed on dendritic cells (56) and binds to Fuc, ManNAc, and D-mannose (Man) in a calcium-dependent manner (13, 57). DC-SIGN acts as an adhesion molecule but also recognizes a range of endogenous and exogenous ligands such as various pathogens including viruses,

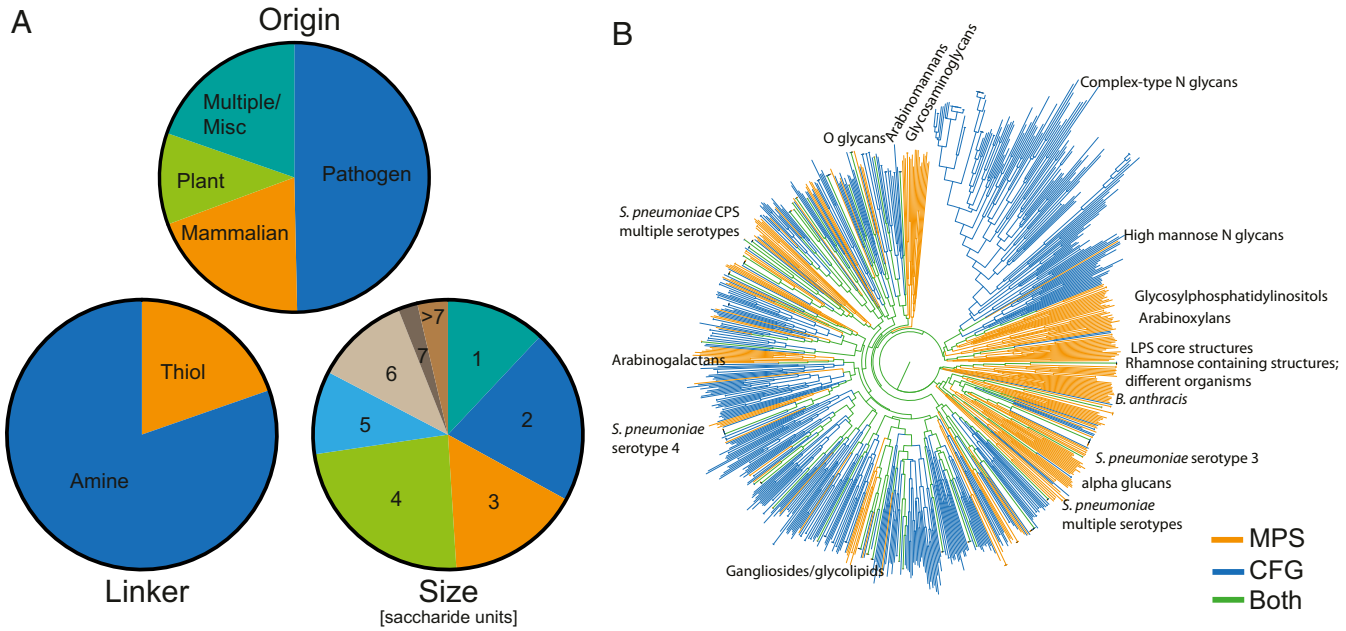

Fig. 3. Analysis of the MPS glycan library (version 2015) for glycan array surface immobilization. (*A*) Distribution of organisms from which the glycans originate, number of glycans equipped with thiol- or aminolinker, and size distribution of glycans. (*B*) Clustering of compounds of the MPS library and the set immobilized on the CFG mammalian array according to glycan similarity (45). Each line terminus represents one glycan with MPS glycans colored in orange, CFG in blue, and structures contained in both sets as well as inner branches leading to structures of both sets colored in green.

fungi, bacteria, and protozoa (56, 58). Two DC-SIGN constructs were screened on the 140-compound glycan array: the tetrameric DC-SIGN-T in which the extracellular domain (ECD) was overexpressed in *Escherichia coli* (59) and the dimeric binder DC-SIGN-D obtained by fusion of the DC-SIGN ECD to the heavy-chain constant region of human IgG1 followed by expression in CHO-S cells (60, 61). The two constructs showed very similar patterns of glycan recognition (Fig. 5 and *SI Appendix*, Figs. S5–S11). Binding was dependent upon Ca^{2+} as EDTA led to complete signal abrogation. Major ligands were the Lewis antigens Le^A **158**, Le^B **159**, Le^X **154** and **176**, and Le^Y **157**, in good agreement with previous findings (58) (Fig. 5 and *SI Appendix*, Figs. S5–S11). Some differences, possibly reduced by binding still close to saturation at this concentration, were visible for the different Lewis antigens at the lowest concentration of DC-SIGN-T (1 μg/mL), with Le^Y **157** being the most tightly bound Lewis glycan. Binding was still saturated for DC-SIGN-D at the same concentration. The differences, also only observed for 1 μg/mL DC-SIGN-T, between the two Le^X constructs **154** and **176**, the only Lewis antigen with a different linker, can be attributed to the impact of the linker structure on surface glycan presentation and interactions with the GBP (62).

Both DC-SIGN-D and DC-SIGN-T recognize three ManNAc-terminating oligosaccharides from *Streptococcus pneumoniae* including serotype 4 CPS repeating unit tetrasaccharide **219** as well as tetrasaccharide **74** that lacks the immunodominant rare pyruvate ketal (63, 64). Failure of the DC-SIGN constructs to bind trisaccharide **77**, which is **74** lacking the terminal ManNAc, suggests that this interaction is mediated by this high-affinity ligand of DC-SIGN (65). Recognition of *S. pneumoniae* serogroup 9 trisaccharide **243**, but not the whole repeating unit of serotype 9A pentasaccharide **239**, suggests that the binding site may be blocked in the natural polysaccharide (Fig. 5 and *SI Appendix*, Fig. S5).

As expected from the monosaccharide specificity of DC-SIGN, the DC-SIGN-D and DC-SIGN-T constructs bound to several glycans with terminal Man moieties, of which recognition of α(1,2) linked mannosides **83** and **85** appeared strongest (Fig. 5 and *SI Appendix*, Figs. S5–S11). Binding is lower for *Leishmania* lipophosphoglycan capping tetrasaccharide **82** comprising trimannoside **83** with an additional Gal residue β(1,4) linked to the reducing end Man, which is probably due to steric constraints imposed by the additional monosaccharide that reduce binding to the terminal group. As Gal is only a very weak ligand of DC-SIGN (K_d = 72 ± 5 mM) (65), binding to this additional monosaccharide likely cannot compensate for the loss of affinity to Man. Tetrasaccharide **250** is identical to **82** but anchored to the surface by a shorter linker; it is recognized slightly more weakly, probably because the shorter linker impairs accessibility (*SI Appendix*, Figs. S6–S11; see Dataset S5 for a table listing intensities for glycans that are identical except for the linker for all experiments) (62). In a manner similar to **82**, branching appears to impede binding to the terminal Man in glycans **226** and **231** that are substructures of *Toxoplasma gondii* glycosylphosphatidylinositols (Fig. 5 and *SI Appendix*, Fig. S5) (21). Binding is apparent but further decreased when the terminal Man is modified with phosphoethanolamine (glycans **227**, **230**, and **232**; see *SI Appendix*, Figs. S6–S11). In addition to the *Leishmania* and *T. gondii* glycans, specific interaction was also seen with *M. tuberculosis* arabinomannan hexasaccharide **257** (66).

Several LPS core glycans were specifically recognized by the DC-SIGN constructs and the data suggest that the interaction is mediated by a terminal L-glycero-D-mannoheptose (Hep) moiety. Mono-Hep **100** was recognized by both DC-SIGN constructs with intensities similar to mono-Man **237** (Fig. 5 and *SI Appendix*, Fig. S5). Binding strength depends upon the linkage of the terminal Hep residue as well as the overall glycan sequence, with the pattern corresponding well between DC-SIGN-T and DC-SIGN-D. Recognition of tetrasaccharide **95** with a terminal α(1,2) linked Hep was most efficient among all investigated LPS core glycans and significantly greater than that of oligosaccharide **94**, which terminates with α(1,7) linked Hep but is otherwise identical. Several LPS core glycans show intermediate recognition with intensities between those of **94** and **95**, the greatest among these being α(1,3) linked di-Hep **178**. Addition of saccharides to **178**, a Kdo unit in trisaccharide **92** and a Kdo as well as an Ara4N branch in tetrasaccharide **93**, leads to decreased

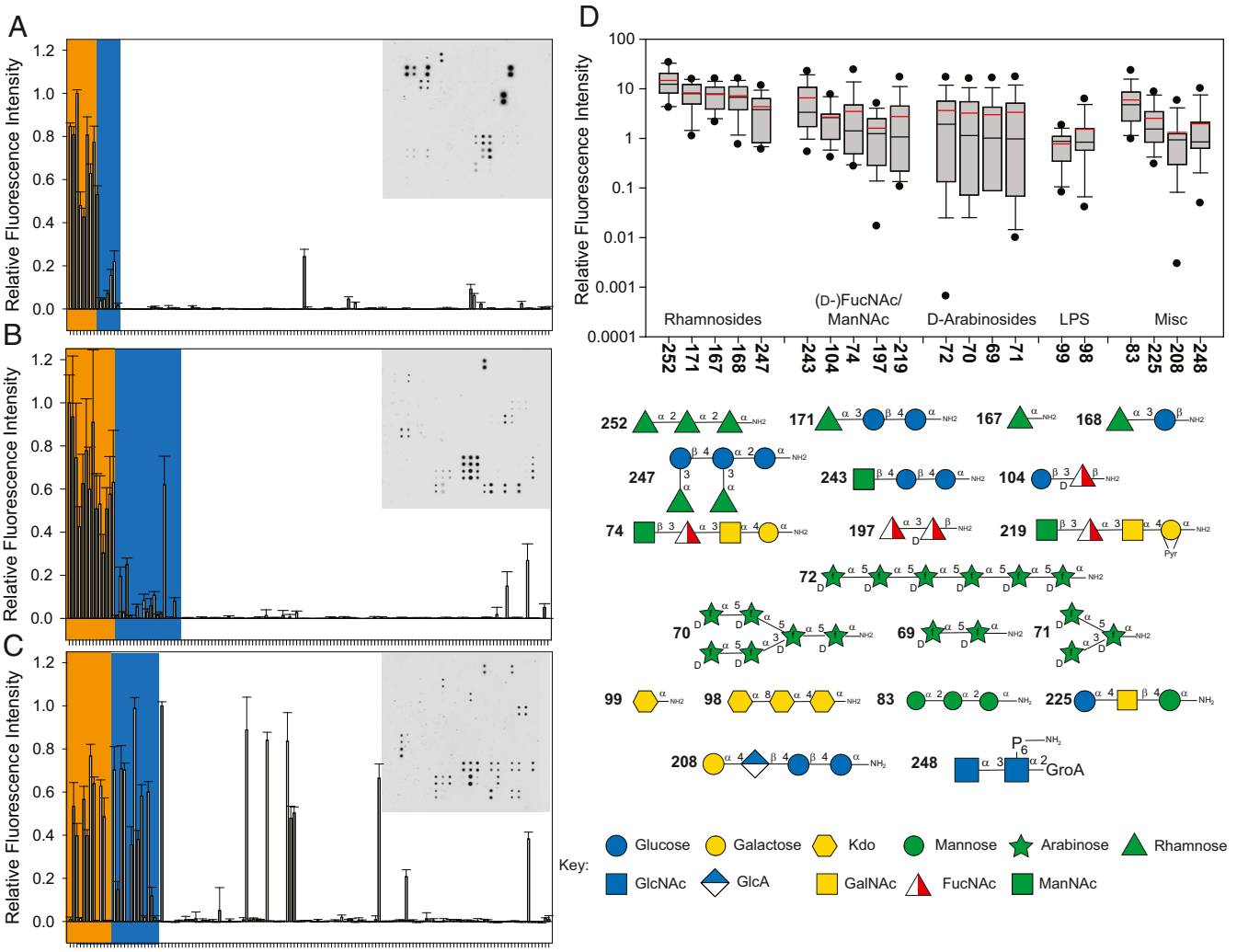

Fig. 4. Quality control of printed glycan arrays with known GBPs and analysis of healthy human sera. (*A*–*C*) Binding pattern of plant lectins Con A (ConA, *A*), soybean agglutinin (SBA, *B*), and WGA (*C*) on a glycan array printed with 140 amino-linked glycans. Compounds are arranged to separate expected binders (left, orange and blue background) from glycans with no known specificity for the respective lectin. Each data point is the mean of four spots from two independent experiments normalized to the strongest bound glycan with error bars representing the SD. Groups of theoretical binders are presented with differently colored background (see *SI Appendix* for details). The same graphs with additional peak annotations as well as binding data from additional plant lectins are depicted in *SI Appendix*, Fig. S2. (*D*) Compounds on the same glycan array that had the highest median signals for IgG binding from $n = 15$ sera of healthy human subjects at a 1:100 dilution. Each data point is the mean of four spots from two independent experiments normalized to the mean binding signal of each experiment. The black bar indicates the median, the red bar the mean intensity, the boxes and whiskers contain the values between the 25th and 75th (boxes) and 10th and 90th percentile (whiskers), and the black dots represent values outside the whisker range. The whole glycan panel is shown in *SI Appendix*, Fig. S4. Graphical representations of glycan structures follow the guidelines of the third edition of *Essentials of Glycobiology* (89).

intensities. Additionally, trisaccharide **97** lacking Kdo but containing one additional Hep was bound stronger than **94** that is identical to **97** but bears a reducing end Kdo. Heavily truncated Hep-Kdo disaccharide **96** is bound to a low level similar to **94**. LPS compounds without Hep were not recognized (**98**, **99**), as were glycans where Hep was capped with GlcNAc (**91**, **177**).

Surface plasmon resonance (SPR)-based interaction studies were used to confirm DC-SIGN-T interaction with heptosides. Di-Hep **178**, a heptoside that is strongly bound on glycan arrays, was immobilized on the SPR chip and DC-SIGN-T was flowed above the surface. The apparent dissociation constant (K_d) of the multimeric interaction was determined to be in the high nanomolar range (*SI Appendix*, Fig. S12) and lower than published low-nanomolar interactions with mannose–BSA conjugate (65).

The MPS glycan library is suitable for identifying new microbial ligands for mammalian lectin immune receptors, as illustrated by the interaction between DC-SIGN and heptosides.

Bacterial Lectins. Pathogens express not only glycans that interact with mammalian GBPs but also numerous lectins with various functions. Bacterial GBPs specific for mammalian glycans mediate host-cell adhesion (67). *Burkholderia cenocepacia* expresses several homologs of *Pseudomonas aeruginosa* LecB, a lectin and virulence factor involved in biofilm formation (68). Two such homologs, BC2L-A and the C-terminal domain of BC2L-C (BC2L-C-ct), are known to bind carbohydrates bearing terminal Man and Hep but had not previously been analyzed using Hep-containing glycan arrays (14, 15, 69). Using the MPS glycan library it is apparent that BC2L-A and BC2L-C-ct specifically bind glycans terminating with Man or the rare sugar Hep (70, 71), while binding to other glycans is minimal (Fig. 6 and *SI Appendix*, Fig. S13). The interactions of BC2L-A and BC2L-C-ct with heptosides and mannosides are calcium-dependent as binding was abrogated in the presence of EDTA. Highest intensities were observed for branched arabinomannan hexasaccharide **257**

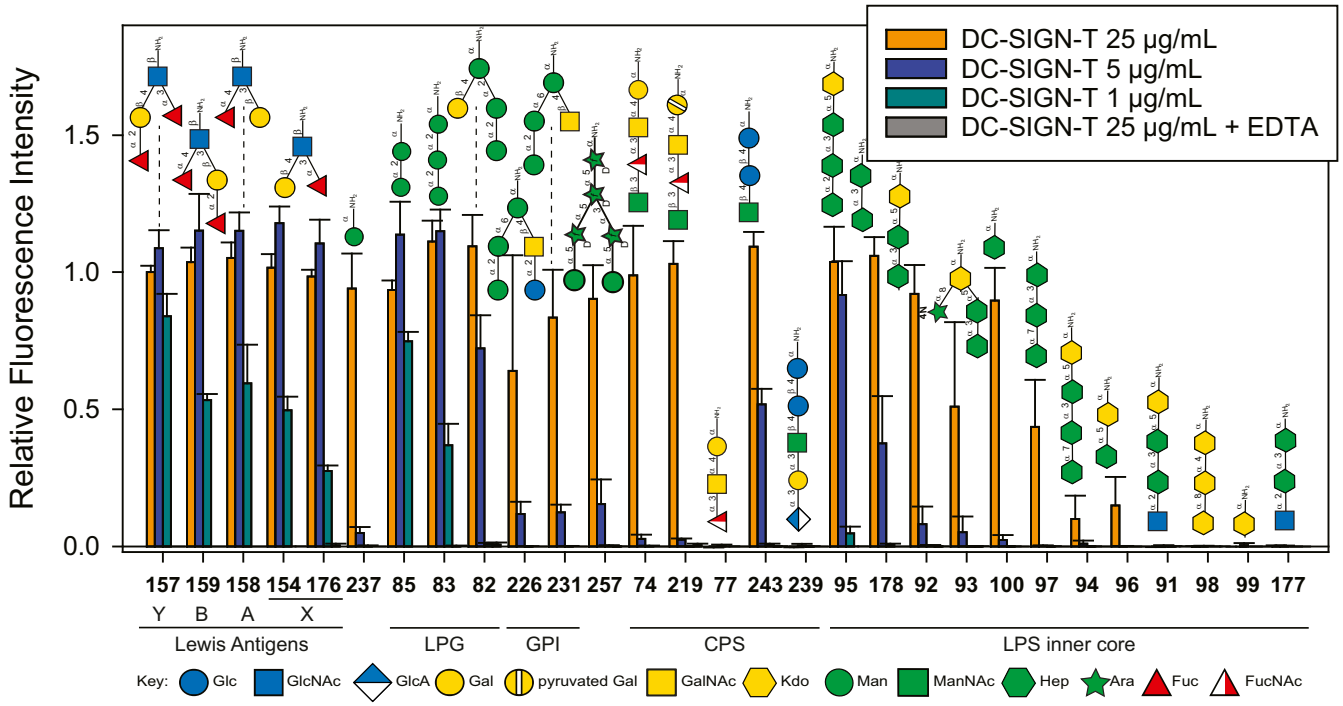

Fig. 5. Analysis of binding specificities of immune lectin receptor DC-SIGN-T on a 140-compound glycan array. Recombinant DC-SIGN-T was screened at the indicated concentrations. Binding toward selected glycan groups, normalized to the signal of Le^Y antigen **157** at a concentration of 25 μg/mL, is shown. Error bars represent SD of four spots derived from two glycan array experiments. The remaining glycan panel is shown in *SI Appendix*, Figs. S6–S8.

that presents two mannose termini. Fluorescence intensities of more weakly bound glycans relative to **257** varied greatly between lectins and glycans but were generally higher for BC2L-C-ct. Comparison of heptose containing glycans suggests that for both lectins a Kdo residue at the reducing end is detrimental (signal intensities: **178** > **92** and **97** > **94**) and that the lectins prefer to bind α(1,7) linked Hep over α(1,2) linked Hep (signal intensities: **94** > **95**). Strong interactions with mannosides and several heptosides allowed for the calculation of surface K_d values for both lectins from the respective concentration series (Fig. 6 and *SI Appendix*, Table S5). Generally, BC2L-A exhibits considerably lower K_d values for mannosides than does BC2L-C-ct (e.g., 0.14 ± 0.02 μM vs. 2.6 ± 0.6 μM, respectively, for dimannoside **85**) while heptoside avidities are within similar ranges when the two lectins are compared (e.g., 5.5 ± 2.7 μM vs. 5.2 ± 0.7 μM, respectively, for diheptoside **178**). K_d value estimation failed for weaker binding glycans, either because of too low fluorescence intensities, even at the highest lectin concentrations, or because the K_d values were outside the range that could be uniquely determined from a concentration series up to 2 mg/mL (*SI Appendix*, Table S5). Where avidities could be estimated, binding strength rankings based on avidities or fluorescence intensities at 1 mg/mL or 0.4 mg/mL correlated well (*SI Appendix*, Table S5). The in-depth analysis of *Burkholderia* lectin glycan specificities highlights the utility of the MPS glycan library for the characterization of microbial virulence factors.

Discussion

Glycan arrays have been a standard method for GBP analysis for over a decade. Several well-characterized collections containing hundreds of glycans that can be immobilized on microarray slides are being curated (4). Few (sub)collections of microbial glycans exist as most synthetic glycan collections focus on mammalian structures. Alternatively, pathogen-focused glycan arrays exposing isolated polysaccharides or shotgun glycan arrays have been described (32, 34, 72). The diversity of microbial carbohydrates that contain many different monosaccharides (7) has rendered the design of a concise microbial glycan array containing pure synthetic glycans challenging. We combined different synthetic techniques (Fig. 1) to prepare a diverse collection of glycans based on many monosaccharide building blocks. The MPS glycan library, the CFG mammalian array (version 5.2), and the Feizi laboratory library have identical diversity scores even though the latter two contain more than twice as many compounds. The libraries differ in focus and overlap only minimally as demonstrated by cluster analysis, thus making them highly complementary (Fig. 3*B* and *SI Appendix*, Fig. S1). The utility of the MPS glycan library is illustrated here with studies in glycoimmunology and the glycobiology of infectious diseases that are based on an array of 140 synthetic glycans.

Glycan immobilization on this array was verified using plant lectins with known specificities for terminal mammalian-type mono- and oligosaccharides, and a high degree of recognition for the glycans that were expected to be bound was observed (Fig. 4 and *SI Appendix*, Figs. S2 and S3 and Tables S1 and S2). Interestingly, binding signals for some glycans were observed where recognition was likely mediated by previously unknown interactions between the lectins and nonmammalian monosaccharides. Namely, the binding of D-FucNAc by lectins DBA, SNL, and WGA is likely a specific interaction as D-FucNAc is the 6-deoxy derivative of the known ligand GalNAc (73, 74) (see label **F1** in *SI Appendix*, Fig. S2). In a similar manner, RCA120 appears to recognize D-FucNAc even though GalNAc is described as only a low-affinity ligand (75). UEA I is known to bind Fuc (73) and also seems to tolerate substitutions at C2, as the MPS library array data reveal interactions with FucNAc terminating structures **77**, **81**, and **103** (*SI Appendix*, Fig. S2). Additionally, several glycans, not recognized by plant lectins, were shown to be immobilized using specific monoclonal antibodies. The high degree of binding among the glycans for which quality-control reagents were available demonstrated the readiness of the array for use in studies to identify new ligands.

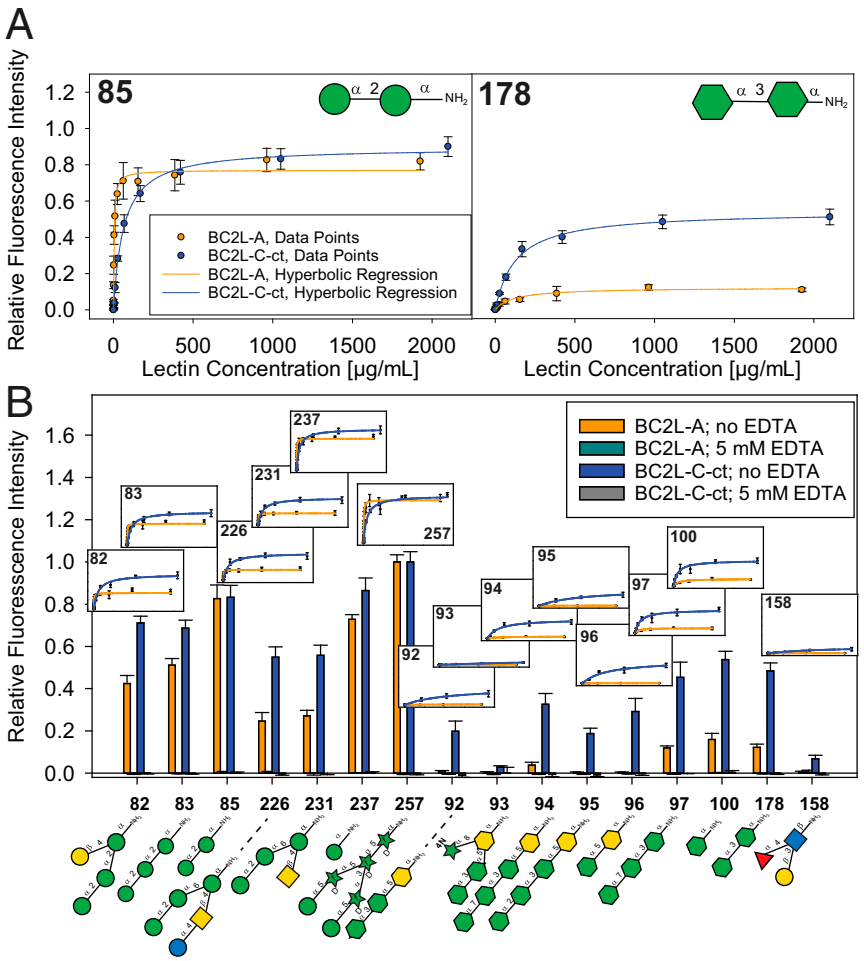

Fig. 6. Analysis of binding specificities of lectins A and C from *B. cenocepacia*. (*A*) Concentration-dependent binding curves of lectins BC2L-A and BC2L-C-ct for a dimannoside and a diheptoside. (*B*) Signal intensities for both lectins at a protein concentration of 1 mg/mL toward all aminopentanol-linked mannosides and heptosides on the array, as well as Le^A trisaccharide **158** as the glycan yielding the greatest intensity for BC2L-C-ct, for comparison. The *Insets* represent concentration-dependent binding curves for all compounds with the same scale as shown in *A*. All values are the mean of six spots from three glycan array experiments and normalized to the signal of the respective lectin toward arabinomannan hexasaccharide **257** at a lectin concentration of 1 mg/mL. Error bars represent SD. The whole glycan panel and representative field images are shown in *SI Appendix*, Fig. S13.

Microbial carbohydrates play a fundamental role in host–microbe interactions. Antibody production against microbial glycans is a key feature of the adaptive immune response (17, 76). Screening of sera from 15 healthy individuals using the validated 140-glycan array identified several glycans with terminal rhamnoses, a microbial sugar known to induce a human immune response (52), that are recognized by antibodies from all tested individuals (Fig. 4*D* and *SI Appendix*, Fig. S4). High antibody levels against glycans containing the nonmammalian monosaccharides FucNAc, D-FucNAc, and ManNAc were observed as well. Only 4 glycans in the top 20 contain exclusively mammalian-type monosaccharides. Three of those are elaborate structures based on pathogen surface components that do not exist in mammals in these monosaccharide and linkage combinations, namely *T. gondii* trisaccharide **225** (21), *S. pneumoniae* tetrasaccharide **208** (77), and *C. difficile* disaccharide **248** (44, 78). The fourth, trimannoside **83**, a substructure of *Leishmania donovani* lipophosphoglycan, can also be found in mammalian glycans. However, as a fragment of larger mammalian structures, the epitope might be distorted so that the antibodies assayed here via microarray would not bind anymore, as has been suggested for antibodies against human epitopes in other glycan array studies (79). Based on the data we present here, we feel confident that this glycan array platform would enable fingerprinting of the immune status of individuals, including chronic infection and immunity due to vaccination, after having been calibrated by large-scale screening of patients with well-documented histories (17, 21).

Most infections are cleared by the innate immune system before specific antibodies against the respective antigen are produced. For that purpose, innate immune cells carry pattern recognition receptors that recognize pathogen-typical molecular patterns (12). CLRs are an important class of pattern-recognition receptors that recognize carbohydrates as foreign or self to activate or inhibit immune cells (80). We screened two recombinant constructs of DC-SIGN, a CLR that is involved in multiple facets of the immune system through its interaction with endogenous and exogenous ligands (56, 58). A CRD Ig-fusion protein (DC-SIGN-D) (60, 61) able to engage in divalent interactions and a tetrameric recombinant ECD (DC-SIGN-T) (59) showed very similar overall glycan recognition. Binding was observed to several glycans terminating with known monosaccharide ligands of DC-SIGN (13, 57, 81), namely Fuc, Man, and ManNAc (Fig. 5 and *SI Appendix*, Figs. S5–S11). Lewis antigens terminating with Fuc were recognized with a preference for Le^Y antigen **157**. ManNAc mediated the interaction with *S. pneumoniae* serotypes 4 and 9 CPS-based oligosaccharides **74**, **219**, and **243** as suggested by the lack of binding to

the very similar glycans **77** and **239**. Mannosides that were identified as interaction partners are also structures based on pathogens, namely *Leishmania* (82), *T. gondii* (21), and *M. tuberculosis* (66).

Most importantly, LPS inner-core glycans presenting terminal Hep were identified as DC-SIGN ligands with α(1,2) and α(1,3) linked Hep being more efficiently bound than α(1,7) linked Hep. GlcNAc capping abrogates binding to α(1,3) linked Hep, suggesting that only terminal Hep is recognized. This finding stands in marked contrast to high-mannose *N*-glycans where DC-SIGN typically binds internal rather than terminal glycan residues (83). Even though DC-SIGN binding to terminal GlcNAc of *LgtB* LPS outer-core mutants of *Neisseria meningitidis* (84) and *Neisseria gonorrhoeae* is observed, GlcNAc monosaccharide alone does not inhibit binding to mannose–BSA conjugates (57). DC-SIGN binds tighter to dimannoside **85** than to LPS core Hep. The L-glyceryl side chain as the main structural difference between D-Man and L,D-Hep may disturb recognition by the DC-SIGN CRD. Satisfyingly, glycan array screening using the MPS library revealed binding events involving DC-SIGN ECD and pathogenic bacteria. The results illustrate the impact of linkages, adjacent glycan residues, and their modifications.

The *B. cenocepacia* lectins BC2L-A and BC2L-C-ct, the C-terminal domain of the "superlectin" BC2L-C, are known to bind to mannosides and heptosides (14, 15, 69). Both lectins are homologs of LecB from *P. aeruginosa* that is known to promote biofilm formation by binding to host tissue receptors (68). BC2L-C is thought to play a role in host-cell adhesion by using the N-terminal domain for binding to host cell glycans while the otherwise soluble lectin stays attached to the bacterium through the C-terminal domain (69). Both BC2L-A and BC2L-C have also been implicated in biofilm formation (14–16). Comparative analyses of BC2L-A and BC2L-C-ct were performed using arrays of glycans terminating with monosaccharides such as Man, Hep, and other rare sugars, and surface dissociation constants for the interaction with glycan ligands were calculated (85). In agreement with the described monosaccharide specificity, binding to terminal mannosides and heptosides was almost exclusively observed (Fig. 6 and *SI Appendix*, Fig. S13). Previously unknown structural features of heptosides that are needed for tight interaction with BC2L-A/C-ct can be inferred, such as the detrimental effects of Kdo in the glycan chain and the preferential recognition of α(1,7) heptoses over α(1,2) heptoses. Reported affinities derived from microcalorimetry measurements show that BC2L-A also prefers α(1,7) linked heptoses over α(1,3) linkages (15). The finding that BC2L-A has higher avidities for mannosides than BC2L-C-ct is consistent with the higher affinities observed by microcalorimetry measurements (15, 69). Avidities for the two lectins toward heptosides were in a similar range, an observation that is in agreement with microcalorimetry measurements on an α(1,3) diheptoside, while monoheptose had been described to be bound more strongly by BC2L-A than BC2L-C-ct in prior work (15, 69). Interestingly, there were no pronounced differences between the lower-affine mannosides and higher-affine heptosides for BC2L-C-ct. This difference had been seen for an α(1,3) diheptoside by microcalorimetry, but potential high-affinity ligands with terminal α(1,7) heptose linkage had not been measured (69).

The concentration series also showed varying fluorescence intensity saturation levels between the different glycans with the intensities at 1 mg/mL giving a good approximation of the saturation levels for the stronger bound glycans (Fig. 6). Different saturation levels had earlier been described as a major hurdle for binding strength determination using glycan arrays, especially when intensities at only a single protein concentration are used as the read-out (38). When comparing calculated saturation levels of heptosides to arabinomannan hexasaccharide **257**, BC2L-A and BC2L-C-ct exhibit notable binding differences: For BC2L-A, saturation levels for heptosides were below 25% of the saturation level of arabinomannan hexasaccharide **257**, while intensities reach levels slightly above 50% for BC2L-C-ct. Dimannoside **85** that, like the heptosides, only has one terminal interacting monosaccharide, reaches ∼80% for both lectins. A combination of several factors including relative speed of dissociation during washing or a mixture of glycan conformations on the surface, not all of which may be bound by both lectins, may be responsible for this observation (62, 86).

In conclusion, we present here a diverse microbe-focused glycan microarray based on synthetic carbohydrates. The extent to which the MPS microbe glycan array could become an essential tool for infectious disease glycobiology has been determined by diversity assessment, validation using plant lectins and monoclonal antibodies, and human serum, human lectin receptor, and bacterial lectin analysis. The results demonstrate that the MPS microbe glycan array has a diversity similar to that of the existing CFG and Imperial College London/Feizi arrays and is highly complementary to those. Validation showed not only the expected binding patterns but also enabled identification of previously unreported plant lectin–microbial glycan binding events, supporting the argument that an array of this kind may open up new avenues of research. Satisfyingly, we found that the MPS glycan library is suitable for studying molecules of both the innate and the adaptive immune system. This was illustrated for the innate immune system by the interaction between DC-SIGN and heptosides and for the adaptive immune system by the recognition of many microbial surface glycans by serum antibodies. In addition, an in-depth analysis of two *Burkholderia* lectins points to the suitability of the library for studying the receptors of pathogens that act as virulence factors. The MPS microbe glycan array screening resource is made available to researchers interested in microbial glycobiology, in particular, or advancing our understanding of glycan-protein interactions, in general. A website (www.mpikg.mpg.de/Glycan-Array-Screening-Facility) has been created so that requests can be made to access our glycan array platform in the context of collaborative efforts.

Materials and Methods

This section contains an overview of the employed methods. Refer to *SI Appendix* and Datasets S1–S5 for details.

Glycan Array Printing. Glycan arrays of 140 aminolinker-containing glycans (*SI Appendix*, Table S2) were obtained by printing on NHS-functionalized glass slides using a robotic noncontact spotter as described previously (63, 64, 71). After quenching unreacted NHS esters with ethanolamine, the slides were washed, dried, and stored at 4 °C. Reporting on glycan array procedures and experimental data in this publication is in accordance with the guidelines laid out by the MIRAGE (minimal information required for a glycomics experiment) initiative (87).

Recombinant Protein Expression. IgG-Fc fusion protein DC-SIGN-D was expressed in CHO cells and purified using Protein G affinity chromatography as described previously (61). ECD tetramer DC-SIGN-T was overexpressed in *E. coli* as inclusion bodies, refolded, and purified by multistep column chromatography as described previously (59).

Proteins BC2L-A and BC2L-C-ct were produced in *E. coli* BL21(DE3) as previously described (14, 69). Lectins were purified by D-mannose-agarose affinity chromatography, dialyzed, freeze-dried, and subsequently labeled with FITC.

General Procedure for Glycan Array Incubations. Slides were blocked with a BSA-containing blocking buffer (except for *Burkholderia* lectins), washed, and dried. A 16-well incubation grid was attached, and serum/lectin dilutions in corresponding buffers were applied. Wells were washed after incubation. If no detection reagent was necessary (plant lectins and *Burkholderia* lectins), the multiwell grid was removed and the slides were washed again and scanned. If detection reagents like secondary antibodies were necessary, these were applied to the single wells. After final incubation, the slides were washed, dried, and scanned. GenePix Pro-7.2 software was used for intensity evaluation. Glycan array data are available in Datasets S1–S5.

SPR Measurements. For avidity measurements on a Biacore T100 instrument, disaccharide **178** was covalently immobilized on a C1 chip using the aminolinker with NHS chemistry and PEG as spacer. DC-SIGN-T was flowed over the derivatized surface and binding as arbitrary response units was evaluated with a thermodynamic binding model using the Biacore T100 software.

Glycan Diversity Analysis. Library diversity was calculated using a published algorithm (45).

ACKNOWLEDGMENTS. We thank Prof. Ten Feizi, director of the Glycosciences Laboratory at Imperial College London, for cooperation and support and coworkers, especially Microarray Project Leader Dr. Yan Liu, in enabling library comparison; Dr. Lenka Malinovska for providing fluorescently labeled *Burkholderia* lectins for initial exploratory studies; all chemists involved in preparing the many defined glycans displayed on the array; and Dr. Allison Berger and Dr. Benjamin Schumann for critically editing the manuscript. Healthy human serum samples were a kind gift of Dr. Andreas Bergmann (Sphingotec GmbH). This work was supported by the Max Planck Society, Zukunftsfonds Berlin, European Regional Development Fund Grant GlyCarDiag, European Research Council Advanced Grant AUTOHEPARIN, German Federal Ministry for Education and Research Grant 0315447, and the Körber Foundation. A.R. was supported by a graduate fellowship of the Studienstiftung des Deutschen Volkes. C.R. is supported by the German Research Foundation through Emmy Noether Fellowship RA1944/2-1, B.L. by Deutsche Forschungsgemeinschaft Grant LE 2498/6-1, and M.T., F.F., B.L., and J.M. by the European Union's Horizon 2020 Research and Innovation Program (Marie Sklodowska-Curie Grant 642870, ETN-Immunoshape). Expression and purification of *Burkholderia* lectins was supported by the project CEITEC 2020 (LQ1601) from the Ministry of Education, Youth and Sports of the Czech Republic. For DC-SIGN-T production, this work used the Multistep Protein Purification Platform (MP3) of the Grenoble Instruct Centre (ISBG; UMS 3518 CNRS-CEA-UJF-EMBL) with support from FRISBI Grant ANR-10-INSB-05-02 and GRAL Grant ANR-10-LABX-49-01 within the Grenoble Partnership for Structural Biology. F.F. also acknowledges the support of the French Agence Nationale de la Recheche (ANR) for Glyco@Alps (ANR- 15-IDEX-02).

1. Benoff S (1997) Carbohydrates and fertilization: An overview. *Mol Hum Reprod* 3: 599–637.
2. Regina Todeschini A, Hakomori SI (2008) Functional role of glycosphingolipids and gangliosides in control of cell adhesion, motility, and growth, through glycosynaptic microdomains. *Biochim Biophys Acta* 1780:421–433.
3. van Kooyk Y, Rabinovich GA (2008) Protein-glycan interactions in the control of innate and adaptive immune responses. *Nat Immunol* 9:593–601.
4. Rillahan CD, Paulson JC (2011) Glycan microarrays for decoding the glycome. *Annu Rev Biochem* 80:797–823.
5. Park S, Gildersleeve JC, Blixt O, Shin I (2013) Carbohydrate microarrays. *Chem Soc Rev* 42:4310–4326.
6. Schnaar RL (2015) Glycans and glycan-binding proteins in immune regulation: A concise introduction to glycobiology for the allergist. *J Allergy Clin Immunol* 135: 609–615.
7. Adibekian A, et al. (2011) Comparative bioinformatics analysis of the mammalian and bacterial glycomes. *Chem Sci* 2:337–344.
8. Herget S, et al. (2008) Statistical analysis of the bacterial carbohydrate structure data base (BCSDB): Characteristics and diversity of bacterial carbohydrates in comparison with mammalian glycans. *BMC Struct Biol* 8:35.
9. Palma AS, Feizi T, Childs RA, Chai W, Liu Y (2014) The neoglycolipid (NGL)-based oligosaccharide microarray system poised to decipher the meta-glycome. *Curr Opin Chem Biol* 18:87–94.
10. Smith DF, Cummings RD (2014) Investigating virus-glycan interactions using glycan microarrays. *Curr Opin Virol* 7:79–87.
11. Geissner A, Anish C, Seeberger PH (2014) Glycan arrays as tools for infectious disease research. *Curr Opin Chem Biol* 18:38–45.
12. Takeuchi O, Akira S (2010) Pattern recognition receptors and inflammation. *Cell* 140: 805–820.
13. Lepenies B, Lee J, Sonkaria S (2013) Targeting C-type lectin receptors with multivalent carbohydrate ligands. *Adv Drug Deliv Rev* 65:1271–1281.
14. Lameignere E, et al. (2008) Structural basis for mannose recognition by a lectin from opportunistic bacteria Burkholderia cenocepacia. *Biochem J* 411:307–318.
15. Marchetti R, et al. (2012) Burkholderia cenocepacia lectin A binding to heptoses from the bacterial lipopolysaccharide. *Glycobiology* 22:1387–1398.
16. Beshr G, et al. (2016) Development of a competitive binding assay for the Burkholderia cenocepacia lectin BC2L-A and structure activity relationship of natural and synthetic inhibitors. *Med Chem Commun* 7:519–530.
17. Muthana SM, Gildersleeve JC (2014) Glycan microarrays: Powerful tools for biomarker discovery. *Cancer Biomark* 14:29–41.
18. Kamena F, et al. (2008) Synthetic GPI array to study antitoxic malaria response. *Nat Chem Biol* 4:238–240.
19. Blixt O, Hoffmann J, Svenson S, Norberg T (2008) Pathogen specific carbohydrate antigen microarrays: A chip for detection of Salmonella O-antigen specific antibodies. *Glycoconj J* 25:27–36.
20. Wang D, et al. (2007) Photogenerated glycan arrays identify immunogenic sugar moieties of Bacillus anthracis exosporium. *Proteomics* 7:180–184.
21. Götze S, et al. (2014) Diagnosis of toxoplasmosis using a synthetic glycosylphosphatidylinositol glycan. *Angew Chem Int Ed Engl* 53:13701–13705.
22. Hanashima S, et al. (2015) Defining the interaction of human soluble lectin ZG16p and mycobacterial phosphatidylinositol mannosides. *ChemBioChem* 16:1502–1511.
23. Geissner A, Seeberger PH (2016) Glycan arrays: From basic biochemical research to bioanalytical and biomedical applications. *Annu Rev Anal Chem (Palo Alto Calif)* 9: 223–247.
24. Baader J, et al. (2011) Polysaccharide microarrays with a CMOS based signal detection unit. *Biosens Bioelectron* 26:1839–1846.
25. Thirumalapura NR, Morton RJ, Ramachandran A, Malayer JR (2005) Lipopolysaccharide microarrays for the detection of antibodies. *J Immunol Methods* 298:73–81.
26. Parthasarathy N, et al. (2008) Application of carbohydrate microarray technology for the detection of Burkholderia pseudomallei, Bacillus anthracis and Francisella tularensis antibodies. *Carbohydr Res* 343:2783–2788.
27. Parthasarathy N, DeShazer D, England M, Waag DM (2006) Polysaccharide microarray technology for the detection of Burkholderia pseudomallei and Burkholderia mallei antibodies. *Diagn Microbiol Infect Dis* 56:329–332.
28. Wang D, Liu S, Trummer BJ, Deng C, Wang A (2002) Carbohydrate microarrays for the recognition of cross-reactive molecular markers of microbes and host cells. *Nat Biotechnol* 20:275–281.
29. Feinberg H, et al. (2011) Structural basis for langerin recognition of diverse pathogen and mammalian glycans through a single binding site. *J Mol Biol* 405:1027–1039.
30. Knirel YA, et al. (2014) Human tandem-repeat-type galectins bind bacterial non-βGal polysaccharides. *Glycoconj J* 31:7–12.
31. Palma AS, et al. (2015) Unravelling glucan recognition systems by glycome microarrays using the designer approach and mass spectrometry. *Mol Cell Proteomics* 14: 974–988.
32. Stowell SR, et al. (2014) Microbial glycan microarrays define key features of host-microbial interactions. *Nat Chem Biol* 10:470–476.
33. Song X, et al. (2011) Shotgun glycomics: A microarray strategy for functional glycomics. *Nat Methods* 8:85–90.
34. Song X, Heimburg-Molinaro J, Cummings RD, Smith DF (2014) Chemistry of natural glycan microarrays. *Curr Opin Chem Biol* 18:70–77.
35. Seeberger PH, Werz DB (2007) Synthesis and medical applications of oligosaccharides. *Nature* 446:1046–1051.
36. Lepenies B, Yin J, Seeberger PH (2010) Applications of synthetic carbohydrates to chemical biology. *Curr Opin Chem Biol* 14:404–411.
37. Wang CH, et al. (2013) Synthesis of Neisseria meningitidis serogroup W135 capsular oligosaccharides for immunogenicity comparison and vaccine development. *Angew Chem Int Ed Engl* 52:9157–9161.
38. Wang L, et al. (2014) Cross-platform comparison of glycan microarray formats. *Glycobiology* 24:507–517.
39. Blixt O, et al. (2004) Printed covalent glycan array for ligand profiling of diverse glycan binding proteins. *Proc Natl Acad Sci USA* 101:17033–17038.
40. Ratner DM, et al. (2004) Probing protein-carbohydrate interactions with microarrays of synthetic oligosaccharides. *ChemBioChem* 5:379–382.
41. Matthies S, Stallforth P, Seeberger PH (2015) Total synthesis of legionaminic acid as basis for serological studies. *J Am Chem Soc* 137:2848–2851.
42. Horlacher T, et al. (2010) Determination of carbohydrate-binding preferences of human galectins with carbohydrate microarrays. *ChemBioChem* 11:1563–1573.
43. Schumann B, Pragani R, Anish C, Pereira CL, Seeberger PH (2014) Synthesis of conjugation-ready zwitterionic oligosaccharides by chemoselective thioglycoside activation. *Chem Sci* 5:1992–2002.
44. Martin CE, et al. (2013) Glycan arrays containing synthetic Clostridium difficile lipoteichoic acid oligomers as tools toward a carbohydrate vaccine. *Chem Commun (Camb)* 49:7159–7161.
45. Rademacher C, Paulson JC (2012) Glycan fingerprints: Calculating diversity in glycan libraries. *ACS Chem Biol* 7:829–834.
46. Schumann B, et al. (2018) Development of an efficacious, semisynthetic glycoconjugate vaccine candidate against *Streptococcus pneumoniae* serotype 1. *ACS Cent Sci* 4:357–361.
47. Smith DF, Cummings RD (2013) Application of microarrays for deciphering the structure and function of the human glycome. *Mol Cell Proteomics* 12:902–912.
48. Hirabayashi J, Yamada M, Kuno A, Tateno H (2013) Lectin microarrays: Concept, principle and applications. *Chem Soc Rev* 42:4443–4458.
49. Kearney JF, Patel P, Stefanov EK, King RG (2015) Natural antibody repertoires: Development and functional role in inhibiting allergic airway disease. *Annu Rev Immunol* 33:475–504.
50. Huflejt ME, et al. (2009) Anti-carbohydrate antibodies of normal sera: Findings, surprises and challenges. *Mol Immunol* 46:3037–3049.
51. Martin CE, et al. (2013) Immunological evaluation of a synthetic Clostridium difficile oligosaccharide conjugate vaccine candidate and identification of a minimal epitope. *J Am Chem Soc* 135:9713–9722.
52. Schwarz M, et al. (2003) A new kind of carbohydrate array, its use for profiling antiglycan antibodies, and the discovery of a novel human cellulose-binding antibody. *Glycobiology* 13:749–754.
53. Kubler-Kielb J, et al. (2013) The capsular polysaccharide and lipopolysaccharide structures of two carbapenem resistant Klebsiella pneumoniae outbreak isolates. *Carbohydr Res* 369:6–9.

54. Seeberger PH, et al. (2017) A semi-synthetic glycoconjugate vaccine candidate for carbapenem-resistant Klebsiella pneumoniae. *Angew Chem Int Ed Engl* 56: 13973–13978.
55. Kandasamy J, Hurevich M, Seeberger PH (2013) Automated solid phase synthesis of oligoarabinofuranosides. *Chem Commun (Camb)* 49:4453–4455.
56. Svajger U, Anderluh M, Jeras M, Obermajer N (2010) C-type lectin DC-SIGN: An adhesion, signalling and antigen-uptake molecule that guides dendritic cells in immunity. *Cell Signal* 22:1397–1405.
57. Lee RT, et al. (2011) Survey of immune-related, mannose/fucose-binding C-type lectin receptors reveals widely divergent sugar-binding specificities. *Glycobiology* 21: 512–520.
58. Van Liempt E, et al. (2004) Molecular basis of the differences in binding properties of the highly related C-type lectins DC-SIGN and L-SIGN to Lewis X trisaccharide and Schistosoma mansoni egg antigens. *J Biol Chem* 279:33161–33167.
59. Tabarani G, et al. (2009) DC-SIGN neck domain is a pH-sensor controlling oligomerization: SAXS and hydrodynamic studies of extracellular domain. *J Biol Chem* 284: 21229–21240.
60. Maglinao M, et al. (2014) A platform to screen for C-type lectin receptor-binding carbohydrates and their potential for cell-specific targeting and immune modulation. *J Control Release* 175:36–42.
61. Johannssen T, Lepenies B (2015) Identification and characterization of carbohydrate-based adjuvants. *Methods Mol Biol* 1331:173–187.
62. Grant OC, Smith HM, Firsova D, Fadda E, Woods RJ (2014) Presentation, presentation, presentation! Molecular-level insight into linker effects on glycan array screening data. *Glycobiology* 24:17–25.
63. Pereira CL, Geissner A, Anish C, Seeberger PH (2015) Chemical synthesis elucidates the immunological importance of a pyruvate modification in the capsular polysaccharide of Streptococcus pneumoniae serotype 4. *Angew Chem Int Ed Engl* 54:10016–10019.
64. Geissner A, Pereira CL, Leddermann M, Anish C, Seeberger PH (2016) Deciphering antigenic determinants of Streptococcus pneumoniae serotype 4 capsular polysaccharide using synthetic oligosaccharides. *ACS Chem Biol* 11:335–344.
65. Mitchell DA, Fadden AJ, Drickamer K (2001) A novel mechanism of carbohydrate recognition by the C-type lectins DC-SIGN and DC-SIGNR. Subunit organization and binding to multivalent ligands. *J Biol Chem* 276:28939–28945.
66. Hahm HS, et al. (2017) Automated glycan assembly using the Glyconeer 2.1 synthesizer. *Proc Natl Acad Sci USA* 114:E3385–E3389.
67. Audfray A, Varrot A, Imberty A (2013) Bacteria love our sugars: Interaction between soluble lectins and human fucosylated glycans, structures, thermodynamics and design of competing glycocompounds. *C R Chim* 16:482–490.
68. Tielker D, et al. (2005) Pseudomonas aeruginosa lectin LecB is located in the outer membrane and is involved in biofilm formation. *Microbiology* 151:1313–1323.
69. Sulák O, et al. (2011) Burkholderia cenocepacia BC2L-C is a super lectin with dual specificity and proinflammatory activity. *PLoS Pathog* 7:e1002238.
70. Yang Y, Oishi S, Martin CE, Seeberger PH (2013) Diversity-oriented synthesis of inner core oligosaccharides of the lipopolysaccharide of pathogenic gram-negative bacteria. *J Am Chem Soc* 135:6262–6271.
71. Reinhardt A, et al. (2015) Antigenic potential of a highly conserved Neisseria meningitidis lipopolysaccharide inner core structure defined by chemical synthesis. *Chem Biol* 22:38–49.
72. van Diepen A, et al. (2012) Differential anti-glycan antibody responses in Schistosoma mansoni-infected children and adults studied by shotgun glycan microarray. *PLoS Negl Trop Dis* 6:e1922.
73. Kobayashi Y, Tateno H, Ogawa H, Yamamoto K, Hirabayashi J (2014) *Lectins*, ed Hirabayashi J (Springer, New York), pp 555–577.
74. Wu AM, Wu JH, Song SC, Tsai MS, Herp A (1998) Studies on the binding of wheat germ agglutinin (Triticum vulgaris) to O-glycans. *FEBS Lett* 440:315–319.
75. Wu AM, et al. (2006) Recognition factors of Ricinus communis agglutinin 1 (RCA(1)). *Mol Immunol* 43:1700–1715.
76. Schneider C, et al. (2015) The human IgG anti-carbohydrate repertoire exhibits a universal architecture and contains specificity for microbial attachment sites. *Sci Transl Med* 7:269ra1.
77. Schumann B, et al. (2017) A semisynthetic Streptococcus pneumoniae serotype 8 glycoconjugate vaccine. *Sci Transl Med* 9:eaaf5347.
78. Broecker F, et al. (2016) Synthetic lipoteichoic acid glycans are potential vaccine candidates to protect from Clostridium difficile infections. *Cell Chem Biol* 23: 1014–1022.
79. Bovin N, et al. (2012) Repertoire of human natural anti-glycan immunoglobulins. Do we have auto-antibodies? *Biochim Biophys Acta* 1820:1373–1382.
80. Sancho D, Reis e Sousa C (2012) Signaling by myeloid C-type lectin receptors in immunity and homeostasis. *Annu Rev Immunol* 30:491–529.
81. Zhang F, Ren S, Zuo Y (2014) DC-SIGN, DC-SIGNR and LSECtin: C-type lectins for infection. *Int Rev Immunol* 33:54–66.
82. Anish C, et al. (2013) Immunogenicity and diagnostic potential of synthetic antigenic cell surface glycans of Leishmania. *ACS Chem Biol* 8:2412–2422.
83. Feinberg H, Mitchell DA, Drickamer K, Weis WI (2001) Structural basis for selective recognition of oligosaccharides by DC-SIGN and DC-SIGNR. *Science* 294:2163–2166.
84. Steeghs L, et al. (2006) Neisseria meningitidis expressing lgtB lipopolysaccharide targets DC-SIGN and modulates dendritic cell function. *Cell Microbiol* 8:316–325.
85. Liang PH, Wang SK, Wong CH (2007) Quantitative analysis of carbohydrate-protein interactions using glycan microarrays: Determination of surface and solution dissociation constants. *J Am Chem Soc* 129:11177–11184.
86. Tateno H, et al. (2008) Glycoconjugate microarray based on an evanescent-field fluorescence-assisted detection principle for investigation of glycan-binding proteins. *Glycobiology* 18:789–798.
87. Liu Y, et al. (2017) The minimum information required for a glycomics experiment (MIRAGE) project: Improving the standards for reporting glycan microarray-based data. *Glycobiology* 27:280–284.
88. Shore DA, et al. (2013) Structural and antigenic variation among diverse clade 2 H5N1 viruses. *PLoS One* 8:e75209.
89. Varki A, et al. (2015) Symbol nomenclature for graphical representations of glycans. *Glycobiology* 25:1323–1324.